

Analysis of radial velocity variations in multiple planetary systems

András Pál*

Konkoly Observatory of the Hungarian Academy of Sciences, Konkoly Thege Miklós út 15-17, H-1121 Budapest, Hungary
Department of Astronomy, Loránd Eötvös University, Pázmány P. st. 1/A, Budapest H-1117, Hungary

Accepted Received . . . ; in original form . . .

ABSTRACT

The study of multiple extrasolar planetary systems has the opportunity to obtain constraints for the planetary masses and orbital inclinations via the detection of mutual perturbations. The analysis of precise radial velocity measurements might reveal these planet-planet interactions and yields a more accurate view of such planetary systems. Like in the generic data modelling problems, a fit to radial velocity data series has a set of unknown parameters of which parametric derivatives have to be known by both the regression methods and the estimations for the uncertainties. In this paper an algorithm is described that aids the computation of such derivatives in case of when planetary perturbations are not neglected. The application of the algorithm is demonstrated on the planetary systems of HD 73526, HD 128311 and HD 155358. In addition to the functions related to radial velocity analysis, the actual implementation of the algorithm contains functions that computes spatial coordinates, velocities and barycentric coordinates for each planet. These functions aid the joint analysis of multiple transiting planetary systems, transit timing and/or duration variations or systems where the proper motion of the host star is also measured involving high precision astrometry. The practical implementation related to the above mentioned problems features functions that make these kind of investigations rather simple and effective.

Key words: Celestial mechanics – Methods: Analytical, Numerical – Methods: N -body simulations – Techniques: radial velocities

1 INTRODUCTION

As of this writing, 36 multiple planetary systems are known around main sequence stars. Most of these systems bear two detected planets, 8 of them have 3 and 2 of them have 4 planets while the star 55 Cnc has 5 companions¹. With the exception of HR 8799 (Marois et al. 2008), all of the detections are based on or confirmed by the measurements of the radial velocity (RV) variations of the host stars². The planet HAT-P-13b (Bakos et al. 2009) also transits its host star. The detection of this planet was based on transit photometry while the second companion in this system has been revealed by radial velocity measurements. In general, analysis of RV variations constrains the mass (m) of planets by a lower limit. Namely, only the quantity $m \sin i$ is determined by RV data where i is the orbital inclination (relative to

the tangential plane of sky). With the exception of transiting planets and systems where the spatial motion of the host star is detected via astrometry, there is no direct evidence for the actual value of the orbital inclination (and therefore the mass of the planet). In case of transiting systems, inclinations are constrained by measuring the impact parameter from the light curves (see e.g. Pál et al. 2010), while astrometry yields not only the inclination but the orientation of the orbital plane as well (Bean & Seifahrt 2009; Benedict et al. 2010; McArthur et al. 2010). The planetary system around GJ 876 is the only known one where mutual inclination is also detected with a $2\text{-}\sigma$ confidence (Bean & Seifahrt 2009). A great advantage of multiple planetary systems is the possibility of detecting mutual perturbations via the deflection of RV values from the purely Keplerian solution (see e.g. Laughlin & Chambers 2001). Therefore, precise analysis of accurate RV series may yield to an acceptable constraint for both the inclination and the planetary masses. Additionally, planet-planet interactions depend on the mutual inclinations, thus more complex models (such as non-coplanar orbits) for the whole planetary systems can be investigated.

* E-mail: apal@szofi.net

¹ See e.g. <http://exoplanet.eu> for an up-to-date list.

² The planetary system around HR 8799 with 3 confirmed planets has been detected by direct imaging.

Like in the majority of data modelling problems, RV variations (of the host star) in single or multiple planetary systems are modelled with a function of a few external (unknown) parameters. These parameters include the orbital elements and the masses of the planets as well as the barycentric velocity of the host star. For most of the regression methods involved in data modelling (see e.g. the Levenberg-Marquard algorithm, Press et al. 1992), and for the analytic estimation of the covariances, uncertainties and correlations of the model parameters (see e.g. Finn 1992; Pál 2009a), the partial derivatives of the model functions (with respect to the model parameters) have to be known in advance. The simplest way of RV curve modelling does not take into account the mutual interactions between the planets and characterizes the observed RV variations as a sum of independent Keplerian models. Wright & Howard (2009) describes an algorithm detailing the efficient computation of the parametric derivatives of RV model functions where the mutual planetary perturbations are neglected. The main objective of this paper is to present an algorithm that calculates parametric derivatives when the planet-planet interactions are also taken into account.

The structure of the paper is as follows. In the next section, we describe the mathematical tools used to construct the algorithm itself (including the discussion of optimal orbital parameterization, and the numerical integration). In Section 3 the practical implementation is detailed while in Section 4 we demonstrate the usage of the algorithm for three specific multiple planetary systems. The results are summarized in the last section.

2 ORBITAL PARAMETERIZATION AND NUMERICAL INTEGRATION

In this section we summarize the conventions involved in the orbital parameterizations (as used throughout this paper), the algorithms used for numerical integrations and the methods applied in the calculations of parametric derivatives of the radial velocity model functions.

2.1 Spectroscopic and Keplerian orbital elements

The measured radial velocity variations of the host star determine the *spectroscopic* orbital elements of the planetary companion(s). In the case of a system with a single planet, there are 6 of such parameters: the period, P , the time of periastron passage, T_p , eccentricity, e , argument of periastron, ω , the semi-amplitude of the RV variations, K , and the zero-point (or the mean) radial velocity of the central body, γ . The above set of orbital parameters is the most widely used in the literature, however, it is not the best choice for our purposes because of the following reasons. First, for nearly circular orbits the argument of pericenter is not so well constrained and for exactly circular orbits it cannot be defined at all. Second, the time of pericenter passage is also purely constrained for orbits with small eccentricities and not defined for $e = 0$. In order to avoid such ambiguities, one can use the Lagrangian orbital elements $k = e \cos \omega$ and $h = e \sin \omega$ for the parameterization of the shape of the orbit and use one of the following quantities instead of T_p : the mean longitude $\lambda \equiv \lambda(E_0)$ or the orbital

longitude $\varphi \equiv \varphi(E_0)$ for a certain fixed epoch E_0 , or the moments T_{λ_0} or T_{φ_0} when the mean longitude or the orbital longitude have a certain fixed value of λ_0 or φ_0 , respectively. All of the above four quantities are well-defined for circular and nearly circular orbits. The element T_{φ_0} is widely used in the case of transiting planets since due to the definition of the alignment of the reference frame, transits occur at $\varphi_0 = \pi/2$. In the case of multiple planetary systems where the mutual interactions are not negligible, the usage T_{λ_0} or T_{φ_0} is not the best choice since in practice these imply different epochs for the distinct planets. Throughout this paper, we use the mean longitude λ as the primary orbital element to characterize the phase of the orbital motion. The conversion between T_p and λ is rather simple, namely

$$\lambda = \frac{2\pi}{P} (E_0 - T_p) + \omega. \quad (1)$$

Since the mean longitude at an arbitrary moment t is $\lambda(t) = n(t - E_0) + \lambda$, i.e. it is a linear function of the mean motion $n = (2\pi)/P$ and the λ , we prefer n to P . There is an additional benefit using n for characterizing orbital periods: simple error propagation estimations yield that for a given RV semi-amplitude, the uncertainty of n is independent for n itself. In other words, in a multiple planetary systems where planets have masses with the same magnitude, one can expect that the obtained uncertainties are also roughly the same. This is also confirmed by the demonstration analysis presented here (see Sec. 4.1).

In order to interpret the spectroscopic orbital elements, these should be converted into Keplerian parameters. For any type of orbits, the orbital eccentricity, argument of periastron, and the mean longitude are interpreted in the same way. In the case of planar orbits, semimajor axis a of the orbit and the mass of the planet m are derived from the mean motion n , and the normalized RV semi-amplitude $\mathcal{K} = KJ$, where $J \equiv \sqrt{1 - e^2} = \sqrt{1 - k^2 - h^2}$. Let us denote the mass of the central star by \mathcal{M} . Using Kepler's Third Law and the barycentric velocity of the central body, namely

$$a^3 n^2 = G(\mathcal{M} + m) \quad (2)$$

and

$$\mathcal{K} = an \frac{m}{\mathcal{M} + m}. \quad (3)$$

we obtain for Gm and a :

$$Gm = (G\mathcal{M})F_m \left(\frac{\mathcal{K}^3}{G\mathcal{M}n} \right), \quad (4)$$

$$\begin{aligned} a &= n^{-2/3} \{G\mathcal{M} + Gm\}^{1/3} = \\ &= n^{-2/3} \left\{ G\mathcal{M} \left[1 + F_m \left(\frac{\mathcal{K}^3}{G\mathcal{M}n} \right) \right] \right\}^{1/3}. \end{aligned} \quad (5)$$

Here $F_m(\alpha)$ denotes the solution of the equation

$$\alpha = \frac{x^3}{(1+x)^2}. \quad (6)$$

If $\alpha \geq 0$, the above equation always has a unique solution. Moreover, if $\alpha > 0$, the $F_m(\alpha)$ function behaves analytically and its derivative is

$$\frac{dF_m(\alpha)}{d\alpha} = \frac{[1 + F_m(\alpha)]F_m(\alpha)}{\alpha[3 + F_m(\alpha)]}. \quad (7)$$

The well-known proportionality $\mathcal{K} \propto Gm$ is a direct consequence of $F_m(\alpha) \approx \alpha^{1/3}$ for $\alpha \ll 1$. We note that in the case

of spatial orbits when the orbital inclination i differs from 90° , the gravitational parameter and the semimajor axis are calculated as above, but the normalized RV semi-amplitude is $\mathcal{K} = KJ(\sin i)^{-1}$.

Once the Keplerian orbital elements are derived, the planar coordinates and velocity vector components of the planet can be calculated as

$$\begin{pmatrix} x \\ y \end{pmatrix} = a \left[\begin{pmatrix} c \\ s \end{pmatrix} + \frac{p}{1+J} \begin{pmatrix} +h \\ -k \end{pmatrix} - \begin{pmatrix} k \\ h \end{pmatrix} \right], \quad (8)$$

$$\begin{pmatrix} \dot{x} \\ \dot{y} \end{pmatrix} = \frac{an}{1-q} \left[\begin{pmatrix} -s \\ +c \end{pmatrix} + \frac{q}{1+J} \begin{pmatrix} +h \\ -k \end{pmatrix} \right]. \quad (9)$$

Here $q = e \cos E$, $p = e \sin E$, $c = \cos(\lambda + p)$ and $s = \sin(\lambda + p)$, while E denotes the eccentric anomaly. As it is shown by Pál (2009a), the quantities q , p , c and s are analytic functions of the mean longitude and the Lagrangian orbital elements (k, h) . The observed radial velocity of the central body is then

$$V_r^{(1)} = -\frac{m}{\mathcal{M} + m} (o_x \dot{x} + o_y \dot{y}), \quad (10)$$

where the unity vector (o_x, o_y) shows the direction of the observer. Due to the historical definition of the reference frames used in the astrophysics of binary stars and extrasolar planets, this vector is fixed to be $(o_x, o_y) = (0, 1)$.

2.2 Lie-integration

In this short section we summarize the properties of the numerical integration of ordinary differential equations named Lie-integration. The main feature of the numerical integration based on the Lie-series (Gröbner & Knapp 1967; Hanslmeier & Dvorak 1984; Eggl & Dvorak 2010) is that the solution of the differential equation

$$\dot{\mathbf{x}}_i = f_i(\mathbf{x}), \quad (11)$$

is approximated by its Taylor series up to a finite order. The coefficients for this power series expansion are generated by the Lie-operator

$$L_0 := \sum_i f_i D_i, \quad (12)$$

(where $D_i \equiv \frac{\partial}{\partial x_i}$) with which the solution of equation (11) can be written as

$$\mathbf{x}(t + \Delta t) = \exp(\Delta t \cdot L_0) \mathbf{x}(t) \quad (13)$$

where

$$\exp(\Delta t \cdot L_0) = \sum_{k=0}^{\infty} \frac{\Delta t^k}{k!} L_0^k = \sum_{k=0}^{\infty} \frac{\Delta t^k}{k!} \left(\sum_i f_i D_i \right)^k. \quad (14)$$

The method of Lie-integration is the finite approximation of the sum in the right-hand side of equation (14), up to the order of M . Thus, the solution after Δt time is approximated by

$$\mathbf{x}(t + \Delta t) \approx \left(\sum_{k=0}^M \frac{\Delta t^k}{k!} L_0^k \right) \mathbf{x}(t) = \sum_{k=0}^M \frac{\Delta t^k}{k!} (L_0^k \mathbf{x}(t)). \quad (15)$$

Supposing the coefficients $L_0^k \mathbf{x}(t)$ are computed, the numerical integration itself is straightforward. In practice, the values of these coefficients are computed involving recurrence

relations, i.e. for $n \geq 0$, the $L_0^{n+1} \mathbf{x}(t)$ terms are evaluated using the previously calculated $L_0^k \mathbf{x}(t)$ ($0 \leq k \leq n$) coefficients. For each particular problem, the recurrence relations must be derived properly. For the general N -body problem, these relations are presented in Hanslmeier & Dvorak (1984) while the relations in the cases when the reference frame is fixed to one of the bodies are shown in Pál & Süli (2007).

The computational cost (CPU time) required by the calculation of the $L_0^k \mathbf{x}(t)$ coefficients is definitely larger than the time of evaluating equation (15) (see Pál & Süli 2007). Thus, a great advantage of the Lie-integration is that the stepsize Δt can be altered after the coefficients are evaluated without much of additional cost, and therefore an effective integration method can be implemented with an adaptive stepsize. Moreover, there is an availability of an alternate way of adaptive integration, namely if the stepsize Δt is kept fixed, the integration order M can also dynamically be increased until we reach the desired precision (see also Eggl & Dvorak 2010). More details about the practical implementation are found in Sec.3.1.

2.3 Motion in the reference frame of one of the bodies

In several applications, such as in the description of a planetary system or in perturbation theory, the equations of motion are transformed into a reference frame whose origin coincides with one of the bodies. Practically, this is the body with the largest mass, i.e. in a planetary system it is the host star. Let us define the central body as the body with the index of $i = 0$. Altogether we have $1 + N$ bodies, where the other ones are indexed by $i = 1, \dots, N$. Let us use the relative (non-inertial) coordinates r_{im} and velocities w_{im} (where the second index m refers to the spatial dimension, i.e. $m = 1$ is for the x coordinate, $m = 2$ is the y coordinate and in non-planar problems, $m = 3$ refers to the z coordinate). The equations of motion in a compact form are

$$\dot{r}_{im} = w_{im}, \quad (16)$$

$$\begin{aligned} \dot{w}_{im} &= -G(\mathcal{M} + m_i) \phi_i r_{im} - \\ &- G \sum_{j=1, j \neq i}^N m_j [\phi_{ij} A_{ijm} + \phi_j r_{jm}], \end{aligned} \quad (17)$$

where A_{ijm} is the m th component of the vector pointing from the body j to body i ,

$$A_{ijm} := r_{im} - r_{jm}, \quad (18)$$

ρ_i and ρ_{ij} denotes the distances from the central body and the mutual distances, respectively:

$$\rho_i := \rho_{0i} = \rho_{i0} = \sqrt{\sum_m r_{im} r_{im}}, \quad (19)$$

$$\rho_{ij} := \sqrt{\sum_m A_{ijm} A_{ijm}}, \quad (20)$$

and ϕ_i and ϕ_{ij} are defined as the reciprocal cubic distances,

$$\phi_{ij} := \rho_{ij}^{-3}, \quad (21)$$

$$\phi_i := \rho_i^{-3}. \quad (22)$$

Note that the quantities ρ_i and ρ_{ij} , like so ϕ_i and ϕ_{ij} are distinguished only by the number of their indices. Without going into details, we present the recurrence relations of the Lie-derivatives, including the linearized variables in Appendix A.

Using the notations introduced above, the observed radial velocity is computed as

$$V_r^{(N)} = \sum_m \left(\frac{\sum_{i=1}^N m_i w_{im}}{\mathcal{M} + \sum_{i=1}^N m_i} \right) o_m, \quad (23)$$

where the unity vector $\mathbf{o} \equiv o_m = (o_x, o_y)$ or $o_m = (o_x, o_y, o_z)$ defines the direction of the observer (see also equation 10).

2.4 Parametric derivatives

In the analysis of radial velocity variations in a multiple planetary system, the parametric derivatives of the RV curve have to be computed at a certain moment t with respect to the initial orbital elements (at $t = E_0$). Let us define an arbitrary quantity Q which depends only on the solution of the ordinary differential equation (11), $Q \equiv Q(\mathbf{x}(t)) \equiv Q(\mathbf{x})$. The parametric derivatives of the quantity Q with respect to the initial conditions $\mathbf{x}^0 \equiv \mathbf{x}|_{t=0}$ can be computed in the following way. First, let us write the linearized equations of equation (11) as

$$\dot{\xi}_k = \xi_m \frac{\partial f_k(\mathbf{x})}{\partial x_m}. \quad (24)$$

(Here and in the following we use the implicit summation notation wherever it is unambiguous.) The variables ξ_k denote the so-called linearized variables for one particular initial condition. Second, due to the linear property, with the solution of the *full linearized* equations

$$\dot{Z}_{\ell k} = Z_{\ell m} \frac{\partial f_k(\mathbf{x})}{\partial x_m}, \quad (25)$$

one can compute the solution of equation (24) for any arbitrary initial conditions ξ_k^0 , namely:

$$\xi_k(t) = Z_{k\ell}(t) \xi_\ell^0 \quad (26)$$

if the respective initial conditions of equation (25) are

$$Z_{\ell k}|_{t=0} = \delta_{\ell k} = \begin{cases} 1 & \text{if } \ell = k, \\ 0 & \text{if } \ell \neq k. \end{cases} \quad (27)$$

Finally, without going into the details, it can be shown that the partial derivatives of $Q(t)$ with respect to the initial conditions $\mathbf{x}^0 \equiv \mathbf{x}|_{t=0}$ is

$$\frac{\partial Q(t)}{\partial x_\ell^0} = Z_{\ell k}(t) \frac{\partial Q}{\partial x_k}. \quad (28)$$

where $Z_{\ell k}(t)$ represents the solution of equation (25) at the instance t . If the initial conditions \mathbf{x}^0 are defined with an alternative parameterization, i.e. $\mathbf{x}^0 = \mathbf{x}^0(\hat{\mathbf{x}})$, the parametric derivatives of the quantity Q with respect to the $\hat{\mathbf{x}}$ are calculated involving the chain rule, namely

$$\frac{\partial Q}{\partial \hat{x}_\ell} = \frac{\partial x_\ell^0}{\partial \hat{x}_m} Z_{mk} \frac{\partial Q}{\partial x_k}. \quad (29)$$

In the analysis of RV data series, $\hat{\mathbf{x}}$ represents the set of spectroscopic orbital elements – including the (normalized) RV semi-amplitude, $\hat{\mathbf{x}} \equiv (\mathcal{K}_i, n_i, \lambda_i, k_i, h_i)$ –, \mathbf{x}^0 represents the spatial coordinates, velocities³ and the gravitational parameters of the planets, while $Q \equiv V_r^{(N)}$, the observed radial velocity. In practice, the partial derivatives $\frac{\partial x_\ell^0}{\partial \hat{x}_m}$ can be computed using the formulae presented in Appendix B, while the computation of the terms $\frac{\partial Q}{\partial x_k}$ is relatively simple since in the equation for the radial velocity (see equation 10 or later in Sec. 2.3, equation 23) is a rational expression of two functions in that are linear with respect to both the coordinates and masses.

2.5 Linearized equations

As we have seen before (Sec. 2.4), linearized equations have to be solved in order to calculate the partial derivatives of an arbitrary quantity (that depends on the solution of the original differential equation) with respect to the initial conditions. As it has been shown in Pál & Süli (2007), using the same notations as above the Lie-derivatives of the partial linearized variables ξ_k (see also the previous subsection) can be written as

$$L^n \xi_k = \xi_m D_m L^n x_k = \xi_m D_m L_0^n x_k. \quad (30)$$

Obviously, this formula can be applied to obtain the solution for the full linearized form (see equation 25):

$$L^n Z_{\ell k} = Z_{\ell m} D_m L_0^n x_k. \quad (31)$$

Thus, the solution for equation (31) has to be substituted into equation (28) or (29) in order to obtain the partial derivatives of arbitrary quantities with respect to the initial conditions. The complete set of recurrence relations for the linearized problem is found in Appendix A.

3 IMPLEMENTATION

The algorithm presented in Section 2 has been implemented as an add-on module for the regression analysis and data modelling program `lfrit`⁴ (described briefly in Pál 2009b) in a form of an ANSI C code. Since the application program interface (API) of `lfrit` for this kind of dynamically loaded libraries is rather simple, the source code module can easily be modified for arbitrary purposes, such as inclusion for other kind of C programs or another languages or programming environments that support linking of C modules (e.g., FORTRAN or IDL). The source code is available from the web address <http://szofi.elte.hu/~apal/utlis/astro/nbrv>. A standalone implementation of the Lie-integrator code is also available from the address <http://szofi.elte.hu/~apal/utlis/astro/lieint>, with the same algorithmical features and with an easy user interface for numerical integration and simple stability investigations.

³ See also Sec. 2.3 for further details about the notations used in the description of multiple planetary systems.

⁴ This program is available as a part of the `libpsn` package, see <http://szofi.elte.hu/~apal/utlis/libpsn/>.

Table 1. List of additional modes as implemented in the generic functions `nbrv_2g_N()` and `nbrv_3g_N()`. These functions have 4 or 5 additional parameters (in the respective cases of 2 and 3 dimensional variants) comparing to the pure RV functions (`nbrv_2d_N()` and `nbrv_3d_N()`). The first additional parameter is the “mode flag”, F , an integer between 0 and 3. The second parameter is the body index, k , a non-negative integer less than or equal to N . The other 2 or 3 parameters are the components of the o_m vector. All of the values computed by these functions are *projected* coordinates or velocities: the spatial vectors are multiplied by the o_m components, yielding a scalar product. Thus, in this table such derived coordinates and velocities are referred as “projected coordinates” or “projected velocities”.

Mode (F)	Body index (k)	Result	Interpretation and typical usage
0	0	$V_{r,m}^{(N)} o_m$	Projected velocity of the barycenter with respect to the central body. In case of planetary systems, interpreted as the radial velocity of the host star where the line-of-sight is defined by the o_m vector. If $\mathbf{o} = (0, 1)$ or $\mathbf{o} = (0, 0, 1)$, the results are equivalent with the results of <code>nbrv_2d_N()</code> and <code>nbrv_3d_N()</code> .
0	$1 \leq k \leq N$	$V_{r,m}^{(N,k)} o_m$	Independent components of the projected barycentric velocity. Although only the joint effect of all of the planets in the planetary system can be measured by radial velocity variations, the contribution of each planet to the final RV curve can be analyzed by this way. Due to the mutual perturbations, these velocity components are not strictly periodic and cannot be described only by the orbital elements of the respective planet.
1	0	$B_{r,m}^{(N)} o_m$	Projected coordinates of the barycenter with respect to the central body. In case of planetary systems, these coordinates describes the wobbling of the host star, as it might be detected by precise astrometric measurements.
1	$1 \leq k \leq N$	$B_{r,m}^{(N,k)} o_m$	Independent components of the projected barycentric coordinates. If the complementary inclination for a particular planet is close to zero, the planet transits the host star, yielding a small flux decrease that can be measured. In case of suchtransiting planets, these coordinates determines the magnitude of the transit timing variations due to light-time effects.
2	$1 \leq k \leq N$	$w_{km} o_m$	Projected spatial velocity of the body k . For planets with a nearly edge-on orbit, the tangential acceleration of transiting planets is negligible at the time of the transits. These velocities well constrain the duration of these transits.
3	$1 \leq k \leq N$	$r_{km} o_m$	Projected spatial coordinates of the body k . These coordinates constrain the shape of these possible transit light curves as well as the precise timings of the transits if an orbit is nearly edge-on.

Table 2. Spectroscopic orbital elements for the planetary systems HD 73526, HD 128311, and HD 155358. These orbital elements have been derived from the data available in the literature (see text for further references) and have been used as an initial condition in the fits discussed in this paper. The last column shows the number of available radial velocity data points (the same as involved in the fits).

System	E_0 (BJD)	M_\star/M_\odot	$\mathcal{K}_i \sin i$ (m/s)	$n_i = 2\pi/P_i$ (1/d)	λ_i (rad)	$k_i = e_i \cos \omega_i$	$h_i = e_i \sin \omega_i$	N_{RV}
HD73526	2, 452, 500	1.08	70.0	0.03360	3.902	-0.402	+0.040	31
			61.4	0.01620	4.150	-0.480	-0.080	
HD128311	2, 452, 500	0.84	64.6	0.01370	1.896	-0.090	+0.233	75
			75.1	0.00677	1.500	-0.160	-0.058	
HD155358	2, 453, 500	0.87	34.6	0.03222	0.894	-0.106	+0.035	71
			14.1	0.01185	0.249	+0.027	-0.174	

Table 3. Best-fit spectroscopic orbital elements and their $1\text{-}\sigma$ uncertainties for the planetary systems HD 73526, HD 128311, and HD 155358 derived by the MCMC algorithm under the assumption of coplanar orbits. The median for each probability distribution is treated as a best-fit value. See text for further details.

System	$\mathcal{K}_i \sin i$ (m/s)	$n_i = 2\pi/P_i$ (1/d)	λ_i (rad)	$k_i = e_i \cos \omega_i$	$h_i = e_i \sin \omega_i$	γ (m/s)	$\sin i$
HD73526	65.9 ± 3.8	0.03359 ± 0.00017	3.855 ± 0.046	-0.404 ± 0.045	$+0.069^{+0.047}_{-0.039}$	-33.6 ± 2.4	$0.82^{+0.18}_{-0.14}$
	61.8 ± 0.5	$0.01629^{+0.00018}_{-0.00015}$	4.108 ± 0.076	$-0.503^{+0.044}_{-0.041}$	-0.046 ± 0.046		
HD128311	$49.1^{+9.2}_{-5.9}$	0.01364 ± 0.00012	$1.599^{+0.219}_{-0.188}$	$+0.035^{+0.112}_{-0.098}$	$+0.337^{+0.071}_{-0.079}$	0.9 ± 2.1	$0.8^{+0.2}_{-0.5}$
	73.8 ± 3.1	0.00663 ± 0.00010	1.396 ± 0.046	$+0.142^{+0.093}_{-0.169}$	$+0.063^{+0.065}_{-0.083}$		
HD155358	31.18 ± 0.34	$0.03225^{+0.00024}_{-0.00016}$	0.867 ± 0.064	-0.136 ± 0.039	$+0.041^{+0.043}_{-0.047}$	10.1 ± 1.0	-
	$13.66^{+1.90}_{-1.58}$	$0.01203^{+0.00029}_{-0.00033}$	$0.161^{+0.147}_{-0.169}$	$-0.065^{+0.091}_{-0.118}$	$-0.138^{+0.116}_{-0.179}$		

In practice, this add-on module (named `nbrv.so` on most of the UNIX systems or `nbrv.dylib` on OS/X) registers the functions named `nbrv_2d_N()` and `nbrv_3d_N()` where $\mathbb{N} \equiv N$ is the number of planets in the planetary systems⁵. These functions have $1 + 5N + 1$ or $1 + 7N + 1$ parameters, for the respective cases for the planar (`nbrv_2d_N`) and spatial (`nbrv_3d_N`) problems. The first parameter is the central mass \mathcal{M} (in Solar units), the following $N \times 5$ or $N \times 7$ parameters are the spectroscopic orbital parameters \mathcal{K}_i (in the units of m/s), n_i (in the units of d^{-1}), λ_i (in radians), k_i and h_i . Furthermore, the spatial functions have two additional parameters: the complementary orbital inclination, $\hat{i} \equiv 90^\circ - i$ and the argument of ascending node, Ω , both angles are measured in radians⁶. All of these orbital elements are defined for a certain epoch of E_0 (BJD). The last parameter is the time Δt elapsed from the epoch E_0 , i.e. $\Delta t = t - E_0$. Here i is the index for the actual planet, $1 \leq i \leq N$.

3.1 Adaptive integration

As mentioned earlier, one of the advantages of the Lie-integration is the possibility of the implementation of a two-way adaptation, by varying both the stepsize and the order of the integration. Since the summation of the Taylor-coefficients in equation (15) does not need so much computing time (compared to the evaluation of these coefficients), the stepsize of the integration can easily be altered in order to reach the desired precision. In practice, the adaptive integration is implemented as follows. First, let us define a minimal and maximal order of M_{\min} and M_{\max} . It is easy to see that an initial, nearly optimal stepsize for the integration is $\Delta t_0 \propto n_{\max}^{-1}$, where n_{\max} is the maximum of the mean motions appearing in the planetary system. In the case of circular orbits, $\Delta t_0 = 0.8 n_{\max}^{-1}$ is a good choice for $M \approx 20$ and for a relative precision of $\delta = 2 \cdot 10^{-16}$. If we allow a minimal and maximal order for the Lie-integration (M_{\min} and M_{\max} , respectively), the adaptive control of the stepsize and integration order is done as:

1. The terms $L_0^k \mathbf{x}$ in equation (15) are evaluated using the appropriate recurrence relations and the summation is performed with a fixed value of Δt .

2. If the desired precision δ is reached before the order of $M = M_{\min}$, Δt is multiplied by the factor M_{\max}/M_{\min} and re-compute the sum in equation (15) (with the additional evaluation of the necessary terms where $k > M$). This step is repeated until $M < M_{\min}$.

3. If the desired precision δ cannot be reached until the order of $M = M_{\max}$, divide Δt by the factor of M_{\max}/M_{\min} and re-compute the sum in equation (15). This step is repeated until $M_{\max} < M$.

4. If the desired precision is reached between the orders of M_{\min} and M_{\max} , accept the value of Δt and proceed with the next step of the integration.

⁵ In the current implementation $N \leq 8$, however, the source code can easily be modified to increase the maximum number of planets.

⁶ The complementary angle of the inclination is used for simplicity: the planar functions yields the same values as the spatial ones if these two additional parameters are set to zero.

We have to note that this kind of two-way adaptive integration assures that we definitely obtain the desired precision level *without* the loss of computing time. In the case of more common integrators (like Runge-Kutta or Bulirsch-Stoer methods), the estimation of the accuracy is based on heuristics and it is not checked by these algorithms that the expected precision is really obtained. If it turns out that the stepsize is too large (or other parameter of the integration should be changed), then a total re-computation is needed for these algorithms and we definitely lose the computing time spent on the previous evaluations.

In the actual implementation of the `nbrv` module, δ has been chosen by default to be the precision level of the IEEE double precision (64 bit) floating point number representation, that is $\delta = 2 \cdot 10^{-16}$. Although it is an extreme precision compared to the implied and required precision level for the problem, this precision implies that the whole set of functions implemented in the module can be treated as analytic functions without any side-effects. Additionally, this precision level ensures that there would not be any systematic distortions by varying the samples on the domain of investigations.

3.2 Properties

In the following, we present some properties for these functions. For simplicity, let us denote by \mathbf{S}_i the set of the spectroscopic orbital elements (n_i, λ_i, k_i, h_i) and define $V_r^{(N)}(\cdot) = \text{nbrv}_r(\cdot)$. Since interaction between the planets is relatively small (comparing to the gravitational force of the central star),

$$V_r^{(N)}(G\mathcal{M}, \mathcal{K}_1, \mathbf{S}_1, \dots, \mathcal{K}_N, \mathbf{S}_N, \Delta t) \approx \sum_{i=1}^N V_r^{(1)}(G\mathcal{M}, \mathcal{K}_i, \mathbf{S}_i, \Delta t). \quad (32)$$

It is easy to show that for fixed values of \mathcal{K}_i , the effect of mutual interactions decreases as the central mass increases, namely

$$\lim_{G\mathcal{M} \rightarrow \infty} V_r^{(N)}(G\mathcal{M}, \mathcal{K}_1, \mathbf{S}_1, \dots, \mathcal{K}_N, \mathbf{S}_N, \Delta t) = \sum_{i=1}^N V_r^{(1)}(G\mathcal{M}, \mathcal{K}_i, \mathbf{S}_i, \Delta t). \quad (33)$$

Similarly, scaling of the normalized RV semi-amplitudes yields the same kind of equation:

$$\lim_{\sin i \rightarrow \infty} (\sin i) V_r^{(N)} \left(G\mathcal{M}, \frac{\mathcal{K}_1}{\sin i}, \mathbf{S}_1, \dots, \frac{\mathcal{K}_N}{\sin i}, \mathbf{S}_N, \Delta t \right) = \sum_{i=1}^N V_r^{(1)}(G\mathcal{M}, \mathcal{K}_i, \mathbf{S}_i, \Delta t). \quad (34)$$

Although $|\sin i| \leq 1$ for real orbits, either the above equation or equation (33) can be used to formally decrease the level of interaction between the planets (Laughlin & Chambers 2001). Additionally, the fit of independent Keplerian orbits involving the right-hand side of equation (32) yields good initial conditions for the real problem.

Additionally, using equations (9) and (10), $V_r^{(1)}$ can also be written as

$$V_r^{(1)}(GM, \mathcal{K}_1, \mathbf{S}_1, \Delta t) = \frac{\mathcal{K}_1}{1-q} \left[\cos(\lambda + p) - \frac{k_1 q}{1+J} \right] \quad (35)$$

where $\mathbf{S}_1 = (n_1, \lambda_1, k_1, h_1)$, $\lambda = n_1 \Delta t + \lambda_1$, $p = p(\lambda, k_1, h_1)$, $q = q(\lambda, k_1, h_1)$ and $J = \sqrt{1 - k_1^2 - h_1^2}$. Obviously, $V_r^{(1)}$ does not depend on GM , therefore this argument is only a formal one.

As it is known from the literature of binary stars and hierarchical stellar systems, if $N = 1$, variations in the argument of the ascending node have no observable effect and like so, for two planets, radial velocity variations depend only on the difference $D = \Omega_2 - \Omega_1$ (that also determines the mutual inclination of the two orbit). In general, for all $N \geq 1$, we can state

$$\sum_{k=1}^N \frac{\partial V_r^{(N)}}{\partial \Omega_k} = 0, \quad (36)$$

that is also equivalent for the previously mentioned special cases for $N = 1$ and $N = 2$. One should keep in mind these properties while utilizing the `nbrv_3d_N()` functions for purely radial velocity data.

3.3 Generic functions

Throughout this paper we were focusing on the analysis of radial velocity variations of host stars in (multiple) planetary systems. However, the results of the numerical N -body integrations can be exploited in another aspects of binary and hierarchical stellar systems and extrasolar planet studies – including eclipsing binaries, transiting planets and planetary systems where astrometric information is also available. For instance, using the spatial coordinates r_{km} , one can estimate the moments of eclipses and transits and characterize the shape of the light curves. Similarly, the velocities w_{km} can directly be used to calculate the durations of the eclipses and transits, since at the time of these events, the tangential acceleration of the transiting body is nearly zero, so the tangential velocity computed from w_{km} is a rather good approximation for the reciprocal duration⁷ Obviously, using the capabilities of the program `lfrit`, the knowledge of the velocities and coordinates can be exploited in complex studies where simultaneous fits are performed on, for instance, RV and astrometric data series (McArthur et al. 2010).

First, let us write the independent components of the barycentric coordinate and velocity in the form of

$$B_{r,m}^{(N,k)} = \frac{m_k r_{km}}{\mathcal{M} + \sum_{i=1}^N m_i} \quad \text{and} \quad (37)$$

$$V_{r,m}^{(N,k)} = \frac{m_k w_{km}}{\mathcal{M} + \sum_{i=1}^N m_i}. \quad (38)$$

It can be shown that the projection of the barycentric coordinates to the line-of-sight is proportional to the light-time

⁷ In practice, total transit duration must be computed by taking into account the impact parameter that is derived from the orbital inclination and the alignment of the orbital ellipse. Therefore, the observed duration depends on the r_{km} coordinates as well.

effects, thus in the analysis of timing variations in eclipsing and/or transiting systems, these corrections should also be taken into account. With the terms defined in equation (38), the observed radial velocity of the host star can be written as

$$V_r^{(N)} = \sum_m \left(\sum_{k=1}^N V_{r,m}^{(N,k)} \right) o_m. \quad (39)$$

The independent components $V_{r,m}^{(N,k)}$ show the influence of each body on the final observed radial velocity variations. However, due to the mutual interactions, these functions are not strictly periodic.

In order to analyze the effects discussed above in multiple stellar and planetary systems the module `nbrv.so` implements the functions `nbrv_2g_N()` and `nbrv_3g_N()` (where $N \equiv N$ is the number of planets). These functions have 4 or 5 additional parameters⁸ comparing to the functions `nbrv_2d_N()` and `nbrv_3d_N()`. The first additional parameter is a mode flag, that is used as a selector between the V_r , B_r , w and r quantities. The second additional parameter is the body index k while the last 2 or 3 numbers represent the (o_x, o_y) or (o_x, o_y, o_z) vector. The value computed by the `nbrv_2g_N()` and `nbrv_3g_N()` functions is a scalar product of the quantities r_{km} , w_{km} , $B_{r,m}^{(N,k)}$ and $V_{r,m}^{(N,k)}$ and the o_m vector. The comprehensive list of the modes implemented in the functions `nbrv_2g_N()` and `nbrv_3g_N()` can be found in Table 1.

4 APPLICATIONS

In this section we describe two possible applications of the algorithms presented in this paper. First, we show some examples related to the problem of orbital characterization. In the second part, we describe in brief how optimal observation scheduling can be performed by employing the `lfrit` code and this implementation discussed above.

4.1 Orbital fits

As a demonstration and application of the algorithm described in Sec. 2, we analyze the radial velocity data for the multiple (double) planetary systems HD 73526 (Tinney et al. 2006), HD 128311 (Vogt et al. 2005; Wright et al. 2009) and HD 155358 (Cochran et al. 2007) in the form as it is available from the literature. The objective of our test presented here is to constrain the orbital inclination assuming a planar model for these planetary systems. Coplanar orbits are expected from modelling (Goldreich, Lithwick & Sari 2004) and also confirmed by observations (Solar System or GJ 876, see Bean & Seifahrt 2009). We note here that complex dynamical and stability investigations for multiple planetary systems can also be used to constrain or refine orbital elements (see e.g. Ferraz-Mello, Michtchenko, & Beaugé 2005), imply alternative planetary configurations (Goździewski & Konacki 2006) or rule out small inclinations (in parallel with direct RV data modelling, see e.g. Laskar & Correia 2009).

We employed the method of Markov Chain Monte-Carlo

⁸ In the cases of 2 and 3 dimensional variants, respectively.

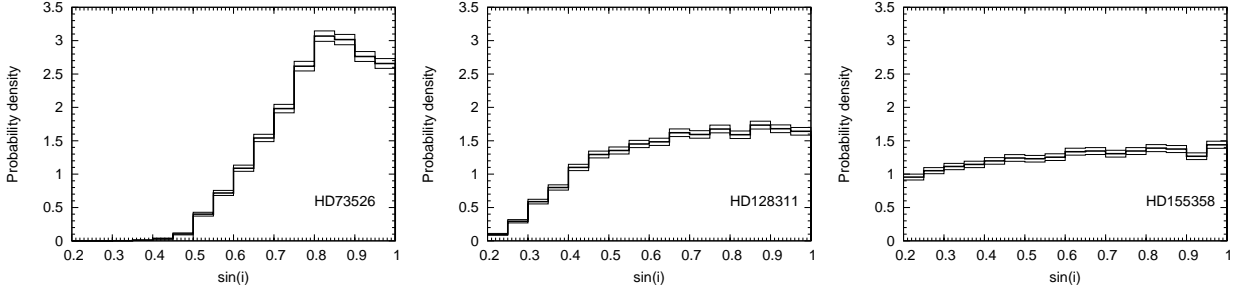


Figure 1. Probability distributions of the $\sin i$ orbital element for the planetary systems HD 73526 (left panel), HD 128311 (middle panel) and HD 155358 (right panel) derived from the radial velocity data available from the literature.

(MCMC, see e.g. Ford 2005) in order to derive the best-fit orbital elements for these interacting planetary systems. The initial conditions (orbital elements) were based on the data available in the literature and summarized in Table 2. This table shows the orbital elements for a certain epoch (E_0) while the eccentricity, argument of pericenter and the time of pericenter passage have been converted to the spectroscopic orbital elements discussed in Sec. 2.1. In all of the fits, the model function

$$RV = \gamma + (\sin i)V_r^{(2)} \left(GM, \frac{\mathcal{K}_1}{\sin i}, \mathbf{S}_1, \frac{\mathcal{K}_2}{\sin i}, \mathbf{S}_2, t - E_0 \right) \quad (40)$$

has been utilized. In the MCMC runs, the values of $\sin i$ have been forced to be between 0.2 and 1 (note the probability that $\sin i$ of a randomly oriented orbit is less than 0.2 is roughly 2%). The results of the fits are displayed in Table 3. The *a posteriori* distributions of the $\sin i$ values are shown in Fig 1. As it is clear from the plots, in the case of HD 73526, the orbital inclination is well defined purely by the RV data, although the upper limit for $\sin i$ is not constrained. Namely, $0.68 \lesssim \sin i$ for this system within $1-\sigma$, that is equivalent with $42^\circ \lesssim i$. For the other two planetary systems, the available RV data do not provide a significant constraint for the inclination.

An advantage of the knowledge of the partial derivatives of the model functions that the uncertainties of the fit parameters can be estimated analytically involving the method of Fisher matrix analysis (Finn 1992; Pál 2009a). We have computed the uncertainties of the $\sin i$ parameters for these planetary systems and obtained $\Delta(\sin i) = 0.19$, $\Delta(\sin i) = 3.87$ and $\Delta(\sin i) = 6.14$ for HD 73526, HD 128311 and HD 155358, respectively. The value for HD 73526 well agrees with the result of the MCMC simulations, while in the case of HD 128311 and HD 155358, these uncertainties are definitely larger than 1, indicating that the amount and/or quality of available radial velocity data is not sufficient for constraining the orbital inclination. Note that in general, Fisher matrix analysis may underestimate the uncertainties if the probability distributions of the fitted variables cannot be approximated by Gaussian distributions. However, in our cases, where the individual measurements are uncorrelated, their formal errors are definitely smaller than the amplitude of the signal and the sampling of the model function is adequate (roughly homogeneous for both periods), such a linear analysis yields reliable results.

The results of this analysis have been compared with the results provided by `Systemic Console` package

(Meschiari et al. 2009) for the planetary system HD 73526. By taking into account the mutual perturbations, the two applications yielded the same values for the best-fit parameters, however, the residual minimization procedure seemed to be more sensitive for the initial parameters in the case of the `Systemic` package. This is mainly due to the inadequate choices of the orbital elements⁹ The uncertainties derived by its built-in bootstrap method were roughly in the same magnitude, however, we were unable to derive such a large set of points that in the case of `lfit/nbrv` since `Systemic` is slower by roughly two orders of magnitude.

4.2 Observation scheduling

Since the program `lfit` is out-of-the-box capable to perform analyses on arbitrary user input for which partial derivatives are known and have an analytic property (thus, it includes the usage of the `nbrv_*()` functions as well), these features can be exploited to optimize observation strategies in order to derive more accurate orbital parameters. Recently, Ford (2008) and Baluev (2008) gives methods with which such strategies can be planned efficiently. As it is known (see these papers), the computation of all of the conditional probabilities, the expected information content (Ford 2008), the D-optimal and L-optimal scheduling instances (Baluev 2008; Pál 2009a) requires the evaluation of the covariance matrices in arbitrary instances. Since the program `lfit` is capable for such an evaluation for arbitrary input functions, with the aid of this program, these computations related to the optimal strategies can be performed as well without any serious difficulties. By default, the program yields both the inverse of the information matrix \mathbf{Q} as defined also by Baluev (2008) and the goodness statistics χ^2 , that and also appears in equations (13) – (15) of Ford (2008). Additionally, `lfit` is capable to perform these kind of linear analyses on arbitrary linear subspace of the parameter domain (i.e. parameters in the orthogonal subspace are assumed to be fixed or known for independent sources), therefore strategies can be built for optimizing various combinations of orbital parameters.

⁹ The `Systemic` package employs mean anomaly, eccentricity and longitude of pericenter instead of mean longitude and Lagrangian elements. A fit performed by `lfit/nbrv` is also more unstable if the former set of orbital elements are used.

5 SUMMARY

In this paper we described an algorithm based on the Lie-integration method that efficiently computes the parametric derivatives of radial velocity model functions for multiple planetary systems when the planet-planet interactions are also taken into account. The analysis of these systems yields more accurate constraints for planetary masses since the orbital and mutual inclinations can also be derived if precise radial velocity data are available. Additionally, the presented analytic formulae and integration method aid to plan observation schedules in order to optimize the telescope time utilization in order to detect planetary perturbations.

ACKNOWLEDGMENTS

The author would thank László Szabados for the careful reading of the draft and for suggestions of improvements and the anonymous referee for further ideas and the careful proofreading. The author would also thank for the numerous discussions with colleagues attended in the Fifth Austrian-Hungarian Workshop on Trojans and Related Topics (Vienna, 2010) that has also been improved the quality of the code. This work has been supported by the scholarship of the Doctoral School of the Eötvös University and also in part by ESA grant PECS 98073.

REFERENCES

- Bakos, G. Á. et al. 2009, *ApJ*, 707, 446
 Bean, J. L. & Seifahrt, A. 2009, *A&A*, 496, 249
 Benedict, G. F., McArthur, B. E., Bean, J. L.; Barnes, R., Harrison, T. E., Hatzes, A., Martioli, E. & Nelan, E. P. 2010, *AJ*, 139, 1844
 Baluev, R. V. 2008, *MNRAS*, 389, 1375
 Borkovits, T., Érdi, B., Forgács-Dajka, E. & Kovács, T. 2003, *A&A*, 398, 1091
 Cochran, W. D., Endl, M., Wittenmyer, R. A. & Bean, J. L. 2007, *ApJ*, 665, 1407
 Eggl, S. & Dvorak, R. 2010, *Lecture Notes in Physics: "An Introduction to Common Numerical Integration Codes Used in Dynamical Astronomy"*, eds. J. Souchay and R. Dvorak, Vol. 790, Springer
 Ferraz-Mello, S., Michtchenko, T. A. & Beaugé, C. 2005, *ApJ*, 621, 473
 Finn, L. S. 1992, *Phys. Rev. D*, 46, 5236
 Ford, E. B. 2005, *AJ*, 129, 1706
 Ford, E. B. 2008, *AJ*, 135, 1008
 Goldreich, P., Lithwick, Y. & Sari, R. 2004, *ApJ*, 614, 497
 Goździewski, K. & Konacki, M. 2006, *ApJ*, 647, 573
 Gröbner, W. & Knapp, H. 1967, "Contributions to the Method of Lie-Series", Bibliographisches Institut, Mannheim
 Hanslmeier, A. & Dvorak, R. 1984, *A&A*, 132, 203
 Kane, S. R., Mahadevan, S., von Braun, K., Laughlin, G. & Ciardi, D. R. 2009, *PASP*, 121, 1386
 Laskar, J. & Correia, A. C. M. 2009, *A&A*, 496, 5
 Laughlin, G. & Chambers, J. E. 2001, *ApJ*, 551, 109
 McArthur, B. E., Benedict, G. F., Barnes, R., Martioli, E., Korzennik, S.; Nelan, E. & Butler, R. P. 2010, *ApJ*, 715, 1203
 Marois, C., Macintosh, B., Barman, T., Zuckerman, B., Song, I., Patience, J., Lafrenière, D. & Doyon, R. 2008, *Science*, 322, 1348
 Meschiari, S., Wolf, A., Rivera, E., Laughlin, G., Vogt, S. & Butler, P. 2009, *PASP*, 121, 1016
 Murray, C. D. & Dermott, S. F. 1999, *Solar System Dynamics*, Cambridge Univ. Press, Cambridge
 Pál, A. & Süli, Á. 2007, *MNRAS*, 381, 1515
 Pál, A. 2009a, *MNRAS*, 396, 1737
 Pál, A. 2009b, PhD thesis (arXiv:0906.3486)
 Pál, A. et al. 2010, *MNRAS*, 401, 2665
 Press, W. H., Teukolsky, S. A., Vetterling, W.T. & Flannery, B.P. 1992, *Numerical Recipes in C: the art of scientific computing*, Second Edition, Cambridge University Press
 Tinney, C. G., Butler, R. P., Marcy, G. W., Jones, H. R. A., Laughlin, G., Carter, B. D., Bailey, J. A. & O'Toole, S. 2006, *ApJ*, 647, 594
 Vogt, S. S., Butler, R. P., Marcy, G. W., Fischer, D. A., Henry, G. W., Laughlin, G., Wright, J. T. & Johnson, J. A. 2005, *ApJ*, 632, 638
 Wright, J. T., Upadhyay, S., Marcy, G. W., Fischer, D. A., Ford, E. B. & Johnson, J. A. 2009, *ApJ*, 693, 1084
 Wright, J. T. & Howard, A. W. 2009, *ApJS*, 182, 205

APPENDIX A: MOTION IN A REFERENCE FRAME FIXED TO ONE OF THE BODIES

Recalling Pál & Süli (2007), Appendix C, the recurrence relations for the N -body problem around a fixed center can be written as

$$L^{n+1}r_{im} = L^n w_{im}, \quad (\text{A1})$$

$$L^n A_{ijm} = L^n r_{im} - L^n r_{jm}, \quad (\text{A2})$$

$$L^n B_{ijm} = L^n w_{im} - L^n w_{jm}, \quad (\text{A3})$$

$$L^n \Lambda_i = \sum_{k=0}^n \binom{n}{k} L^k r_{im} L^{n-k} w_{im}, \quad (\text{A4})$$

$$L^n \Lambda_{ij} = \sum_{k=0}^n \binom{n}{k} L^k A_{ijm} L^{n-k} B_{ijm}, \quad (\text{A5})$$

$$L^{n+1}w_{im} = -G(\mathcal{M} + m_i) \sum_{k=0}^n \binom{n}{k} L^k \phi_i L^{n-k} r_{im} - G \sum_{j=1, j \neq i}^N m_j \sum_{k=0}^n \binom{n}{k} [L^k \phi_{ij} L^{n-k} A_{ijm} + L^k \phi_j L^{n-k} r_{jm}], \quad (\text{A6})$$

$$L^{n+1}\phi_i = \rho_i^{-2} \sum_{k=0}^n F_{nk} L^{n-k} \phi_i L^k \Lambda_i, \quad (\text{A7})$$

$$L^{n+1}\phi_{ij} = \rho_{ij}^{-2} \sum_{k=0}^n F_{nk} L^{n-k} \phi_{ij} L^k \Lambda_{ij}, \quad (\text{A8})$$

where $F_{nk} = (-3)\binom{n}{k} + (-2)\binom{n}{k+1}$. Since the masses (both \mathcal{M} and m_i) are constants, the Lie-derivatives of these are simply $L^{n+1}\mathcal{M} = L^{n+1}m_i = 0$ for $0 \leq n$. Let us denote the linearized of r_{im} , w_{im} , m_i and \mathcal{M} by ξ_{im} , η_{im} , \mathbf{m}_i and \mathfrak{M} , respectively. The vectors Ξ and \mathcal{D} must be extended with the linearized variables \mathbf{m}_i and \mathfrak{M} , namely

$$\hat{\Xi} = (\{\xi_{kp}\}, \{\eta_{kp}\}, \{\mathbf{m}_k\}, \mathfrak{M}) \quad \text{and} \quad \hat{\mathcal{D}} = \left(\left\{ \frac{\partial}{\partial r_{kp}} \right\}, \left\{ \frac{\partial}{\partial w_{kp}} \right\}, \left\{ \frac{\partial}{\partial m_k} \right\}, \frac{\partial}{\partial \mathcal{M}} \right) \quad (\text{A9})$$

and hence

$$\hat{\Xi} \cdot \hat{\mathcal{D}} = \left(\sum_{k,p} \xi_{kp} \frac{\partial}{\partial r_{kp}} \right) + \left(\sum_{k,p} \eta_{kp} \frac{\partial}{\partial w_{kp}} \right) + \left(\sum_k \mathbf{m}_k \frac{\partial}{\partial m_k} \right) + \mathfrak{M} \frac{\partial}{\partial \mathcal{M}}. \quad (\text{A10})$$

It can easily be shown that the complete set of linearized equations extended with the variables \mathbf{m}_i and \mathfrak{M} are

$$L^{n+1}\xi_{im} = L^n \eta_{im}, \quad (\text{A11})$$

$$L^n \alpha_{ijm} = L^n \xi_{im} - L^n \xi_{jm}, \quad (\text{A12})$$

$$L^n \beta_{ijm} = L^n \eta_{im} - L^n \eta_{jm}, \quad (\text{A13})$$

$$\hat{\Xi} \cdot \hat{\mathcal{D}} L^n \Lambda_i = \sum_{k=0}^n \binom{n}{k} (L^k \xi_{im} L^{n-k} w_{im} + L^k r_{im} L^{n-k} \eta_{im}), \quad (\text{A14})$$

$$\hat{\Xi} \cdot \hat{\mathcal{D}} L^n \Lambda_{ij} = \sum_{k=0}^n \binom{n}{k} (L^k \alpha_{ijm} L^{n-k} B_{ijm} + L^k A_{ijm} L^{n-k} \beta_{ijm}), \quad (\text{A15})$$

$$\begin{aligned} L^{n+1}\eta_{im} &= -G(\mathfrak{M} + \mathbf{m}_i) \sum_{k=0}^n \binom{n}{k} L^k \phi_i L^{n-k} r_{im} - G \sum_{j=1, j \neq i}^N m_j \sum_{k=0}^n \binom{n}{k} [L^k \phi_{ij} L^{n-k} A_{ijm} + L^k \phi_j L^{n-k} r_{jm}] - \\ &- G(\mathcal{M} + m_i) \sum_{k=0}^n \binom{n}{k} [(\hat{\Xi} \cdot \hat{\mathcal{D}} L^k \phi_i) L^{n-k} r_{im} + L^k \phi_i L^{n-k} \xi_{im}] - \\ &- G \sum_{j=1, j \neq i}^N m_j \sum_{k=0}^n \binom{n}{k} [(\hat{\Xi} \cdot \hat{\mathcal{D}} L^k \phi_{ij}) L^{n-k} A_{ijm} + L^k \phi_{ij} L^{n-k} \alpha_{ijm} + (\hat{\Xi} \cdot \hat{\mathcal{D}} L^k \phi_j) L^{n-k} r_{jm} + L^k \phi_j L^{n-k} \xi_{jm}], \end{aligned} \quad (\text{A16})$$

$$\hat{\Xi} \cdot \hat{\mathcal{D}} L^{n+1}\phi_i = -2\rho_i^{-2} \xi_{im} r_{im} L^{n+1}\phi_i + \rho_i^{-2} \sum_{k=0}^n F_{nk} [(\hat{\Xi} \cdot \hat{\mathcal{D}} L^{n-k} \phi_i) L^k \Lambda_i + L^{n-k} \phi_i (\hat{\Xi} \cdot \hat{\mathcal{D}} L^k \Lambda_i)], \quad (\text{A17})$$

$$\hat{\Xi} \cdot \hat{\mathcal{D}} L^{n+1}\phi_{ij} = -2\rho_{ij}^{-2} \alpha_{ijm} A_{ijm} L^{n+1}\phi_{ij} + \rho_{ij}^{-2} \sum_{k=0}^n F_{nk} [(\hat{\Xi} \cdot \hat{\mathcal{D}} L^{n-k} \phi_{ij}) L^k \Lambda_{ij} + L^{n-k} \phi_{ij} (\hat{\Xi} \cdot \hat{\mathcal{D}} L^k \Lambda_{ij})]. \quad (\text{A18})$$

Obviously, the auxiliary variables $S_{im}^{[n]}$, $S_{ijm}^{[n]}$, $\Sigma_{im}^{[n]}$ and $\Sigma_{ijm}^{[n]}$ can be introduced as well (see Pál & Süli 2007, Appendix D), in order to optimize the evaluation of equations (A11) – (A18).

APPENDIX B: PARTIAL DERIVATIVES OF THE COORDINATES AND VELOCITIES

The computation of equation (29) requires the partial derivatives of the initial coordinates and velocities with respect to the initial orbital elements. Let us write the initial normalized coordinates and velocities as

$$\begin{pmatrix} \xi \\ \eta \end{pmatrix} = \begin{pmatrix} c \\ s \end{pmatrix} + \frac{p}{1+J} \begin{pmatrix} +h \\ -k \end{pmatrix} - \begin{pmatrix} k \\ h \end{pmatrix}, \quad (\text{B1})$$

$$\begin{pmatrix} \xi' \\ \eta' \end{pmatrix} \equiv \frac{\partial}{\partial \lambda} \begin{pmatrix} \xi \\ \eta \end{pmatrix} = \frac{1}{1-q} \left[\begin{pmatrix} -s \\ +c \end{pmatrix} + \frac{q}{1+J} \begin{pmatrix} +h \\ -k \end{pmatrix} \right] \quad (\text{B2})$$

The normalized coordinates and velocities do not depend on the semimajor axis and the mean motion, therefore these quantities are only functions of the mean longitude λ and the Lagrangian orbital elements (k, h) . In the above equations, $p \equiv p(\lambda, k, h)$, $q \equiv q(\lambda, k, h)$, $c \equiv \cos(p + \lambda)$, $s \equiv \sin(p + \lambda)$ and the quantity J is defined as $J = \sqrt{1 - e^2} = \sqrt{1 - k^2 - h^2}$.

Thus, the partial derivatives of the mass parameter Gm , coordinates (x, y) and velocities (\dot{x}, \dot{y}) with respect to the central mass parameter $G\mathcal{M}$ and the spectroscopic orbital elements – normalized semi-amplitude \mathcal{K} , mean motion n , mean longitude λ and the Lagrangian orbital elements (k, h) – are then

$$\frac{\partial(Gm, x, y, \dot{x}, \dot{y})}{\partial(G\mathcal{M}, \mathcal{K}, n, \lambda, k, h)} = \begin{pmatrix} \frac{2m}{3\mathcal{M} + m} & \frac{3\mathcal{K}^2(\mathcal{M} + m)^3}{n(3\mathcal{M} + m)m^2} & -\frac{\mathcal{K}^3(\mathcal{M} + m)^3}{n^2(3\mathcal{M} + m)m^2} & 0 & 0 & 0 \\ \frac{\partial a}{\partial(G\mathcal{M})}\xi & \frac{\partial a}{\partial \mathcal{K}}\xi & \frac{\partial a}{\partial n}\xi & a\xi' & a\frac{\partial \xi}{\partial k} & a\frac{\partial \xi}{\partial h} \\ \frac{\partial a}{\partial(G\mathcal{M})}\eta & \frac{\partial a}{\partial \mathcal{K}}\eta & \frac{\partial a}{\partial n}\eta & a\eta' & a\frac{\partial \eta}{\partial k} & a\frac{\partial \eta}{\partial h} \\ \frac{\partial a}{\partial(G\mathcal{M})}n\xi' & \frac{\partial a}{\partial \mathcal{K}}n\xi' & \left(a + n\frac{\partial a}{\partial n}\right)\xi' & an\frac{\partial \xi'}{\partial \lambda} & an\frac{\partial \xi'}{\partial k} & an\frac{\partial \xi'}{\partial h} \\ \frac{\partial a}{\partial(G\mathcal{M})}n\eta' & \frac{\partial a}{\partial \mathcal{K}}n\eta' & \left(a + n\frac{\partial a}{\partial n}\right)\eta' & an\frac{\partial \eta'}{\partial \lambda} & an\frac{\partial \eta'}{\partial k} & an\frac{\partial \eta'}{\partial h} \end{pmatrix}. \quad (\text{B3})$$

Here $(\xi', \eta') \equiv \frac{\partial(\xi, \eta)}{\partial \lambda}$ and

$$\frac{\partial a}{\partial(G\mathcal{M})} = \frac{a}{G(3\mathcal{M} + m)} \quad (\text{B4})$$

$$\frac{\partial a}{\partial \mathcal{K}} = \frac{3a\mathcal{K}^2(\mathcal{M} + m)^2}{3nGm^2(3\mathcal{M} + m)} \quad (\text{B5})$$

$$\frac{\partial a}{\partial n} = -\frac{2a}{3n} - \frac{a\mathcal{K}^3(\mathcal{M} + m)^2}{3n^2Gm^2(3\mathcal{M} + m)}. \quad (\text{B6})$$

The partial derivatives of the normalized coordinates (ξ, η) and the normalized velocities (ξ', η') with respect to the orbital elements (λ, k, h) are the following:

$$\frac{\partial(\xi, \eta)}{\partial(k, h)} = \frac{1}{1-q} \left[-\begin{pmatrix} s^2 & -sc \\ -sc & c^2 \end{pmatrix} + \frac{1}{1+J} \begin{pmatrix} sh & -ch \\ -sk & ck \end{pmatrix} \right] + \frac{p}{J(1+J)^2} \begin{pmatrix} kh & h^2 \\ -k^2 & -kh \end{pmatrix} + \begin{pmatrix} -1 & \frac{p}{1+J} \\ -p & -1 \end{pmatrix}, \quad (\text{B7})$$

$$\frac{\partial}{\partial \lambda} \begin{pmatrix} \xi' \\ \eta' \end{pmatrix} = \frac{1}{(1-q)^3} \left[-\begin{pmatrix} c \\ s \end{pmatrix} - \frac{p}{1+J} \begin{pmatrix} +h \\ -k \end{pmatrix} + \begin{pmatrix} k \\ h \end{pmatrix} \right], \quad (\text{B8})$$

$$\begin{aligned} \frac{\partial(\xi', \eta')}{\partial(k, h)} &= \frac{1}{(1-q)^3} \left(\begin{array}{cc} -2sc + ks - qsc + \frac{h(c-k)}{1+J} & c^2 - s^2 + hs - qc^2 + \frac{h(s-h)}{1+J} \\ c^2 - s^2 - ck + qs^2 - \frac{k(c-k)}{1+J} & 2sc - ch - qsc - \frac{k(s-h)}{1+J} \end{array} \right) + \\ &+ \frac{q}{(1-q)J(1+J)^2} \begin{pmatrix} kh & h^2 \\ -k^2 & -kh \end{pmatrix} + \frac{q}{(1-q)(1+J)} \begin{pmatrix} 0 & 1 \\ -1 & 0 \end{pmatrix}. \end{aligned} \quad (\text{B9})$$

This paper has been typeset from a $\text{\TeX}/\text{\LaTeX}$ file prepared by the author.